Airrad Fallout Prediction System

Technical Report

Frederick L. Wasmer
University of Illinois

January 20, 1989

Sponsoring Agencies

Sandia National Laboratories
Albuquerque, NM

U.S. Army Atmospheric Sciences Laboratory
White Sands Missile Range, NM

TABLE OF CONTENTS

LIST OF FIGURES

LIST OF TABLES

LIST OF MAJOR SYMBOLS

A_i = Activity fraction for particle size bin i

$A_{p,i}$ = Total activity associated with a parcel of size bin i, $R \cdot m^2/hr$

A_{tot} = Total activity associated with current event, $R \cdot m^2/hr$

$\cos\theta$, $\sin\theta$ = Cosine and sine of θ, the angle of the major axis of a parcel's distribution measured counterclockwise from east

C_{x0}, C_{y0}, C_{x1}, C_{y1} = Coefficients to transform between grid indices and user coordinates.

$$X = C_{x0} + C_{x1}\, i$$
$$Y = C_{y0} + C_{y1}\, j$$

D_{ij} = Total dose received at grid point [i, j], R

$D_{P,i}$ = Mass-mean diameter of particles of size bin i

$D_{w,i}$ = Wind direction at level i, degrees clockwise from true north

$\bar{f}$ = Average fallspeed of a particle through an atmospheric layer, m/s

F_d = Activity scaling factor for height of burst

$F_{msl,i}$ = Sea level fallspeed of particle of size bin i, m/s

F_{tij} = Value of the [i, j] grid point of the t'th frame grid, R/hr

G = A work grid, defined with same parameters as the frame grids

G_{ij} = Work grid point [i, j]

H_b = Height of burst above ground zero, m

H_{ij} = Value of grid point [i, j] of the hazard indicator under *consideration*

i, j = Indices of a grid point

K = K-factor for the selected fission type, $R \cdot m^2/hr \cdot kt$

N_{cd} = Number of cloud subdivisions: the initial cloud is divided into N_{cd} wafers

n_x, n_y = Number of grid points in x and y directions

$O_{G,x}$, $O_{G,y}$ = User coordinates of the grid origin (point [1, 1]), m east and north

Q = Activity associated with a parcel, $R \cdot m^2/hr$

r = Distance between the ground impact positions of a parcel's bounding particles, m

R_f = Stabilized radius of the fireball, m

R_{H+1} = Activity exposure rate at H+1 hours, R/hr

R_i = Initial radius of the fireball, m

R_s = Disk stabilization radius, m

R_t = Activity exposure rate at time t, R.

$S_{G,x}$, $S_{G,y}$ = Spacing between adjacent grid points in x and y directions, m

$S_{w,i}$ = Wind speed at wind measurement level i, m/s

t, t_1, t_2 = Times since the burst, sec or hr

T_b = Ground impact time of a parcel base, sec since the burst

T_f = Cloud stop time, sec since the burst

$T_{F,1}$ = Frame time of the first (earliest in time) frame grid, sec since the burst.

$T_{F,n}$ = Frame time of the last (latest in time) frame grid, sec since the burst.

$T_{F,t}$ = The frame time of the t'th frame grid, sec since the burst.

T_g = Ground impact time for a parcel, sec since the burst

T_i = Initial fireball time, sec since the burst

$t_{m,B}$ = Time when maximum altitude of the bottom bounding particle of the lowermost parcel is reached, sec since the burst

$t_{m,T}$ = Time when maximum altitude of the top bounding particle of the uppermost parcel is reached, sec since the burst

T_s = Cloud stabilization time, in seconds since the burst

T_t = Ground impact time of a parcel top, sec since the burst

U_w (z) = Function which gives u wind as function of altitude z, m/s

$U_{w,i}$ = U (east) component of wind vector at level i, m/s

V_w (z) = Function which gives v wind as function of altitude z, m/s

$V_{w,i}$ = V (north) component of wind vector at level i, m/s

V_z = Wind speed at height z, m/s

W = Total energy yield, kt

W_f = Fission yield, kt

X, Y = Location of a grid point in user coordinates, m east and north

X_b, Y_b = Ground impact location of a parcel base, m east and north

X_p, Y_p = Location of point half way between the ground impact positions of a parcel's bounding particles, also taken as the center of that parcel's bivariate Gaussian distribution, m east and north

X_t, Y_t = Ground Impact location of a parcel top, m east and north

Z = Height above the ground, m

$Z_{f,B}$ = Stabilized cloud base altitude, m

$Z_{f,T}$ = Stabilized cloud top altitude, m

Z_{gz} = Altitude of ground zero above mean sea level, m

Z_i = Initial altitude of a bounding particle at initial time T_i, m

$Z_{i,B}$ = Initial cloud base altitude, m

$Z_{i,C}$ = Initial cloud center altitude, m

$Z_{i,T}$ = Initial cloud top altitude, m

$z_{m,B}$ = Maximum altitude reached by the bottom bounding particle of the lowermost parcel, m above mean sea level

$z_{m,T}$ = Maximum altitude reached by the top bounding particle of the uppermost parcel, m above mean sea level

Z_p (t) = Function which returns the altitude of a particle as a function of time since the burst, m

Z_s = Altitude at stabilization time T_s of a particle, m

$Z_{s,B}$ = Altitude at stabilization time T_s of a particle initially at the cloud base, m

Z_{scl} = Scaled height of burst, $m/kt^{1/3}$

Z_t = Height of a bounding particle at time t seconds since the burst, m

Δ_{maj} = Component of the distance from the center of a parcel's bivariate Gaussian distribution to a grid point, parallel to the distribution's major axis, m

Δ_{min} = Component of the distance from the center of a parcel's bivariate Gaussian distribution to a grid point, parallel to the distribution's minor axis, m

ΔX = East-west component of r, m

ΔY = North-south component of r, m

ε = Turbulence energy dissipation rate, m^{-1}

θ = The angle of the major axis of a parcel's distribution, measured, ° counterclockwise from east

$\sigma\ (t)^2$ = Variance of a disk as a function of time, m^2

σ_I^2 = Disk variance when its dispersion rate becomes constant ($10^9\ m^2$).

σ_b = Standard deviation of a parcel base, m

σ_G = Standard deviation of a disk at ground impact, m

σ_{maj} = Standard deviation of a parcel's bivariate Gaussian distribution along the major axis, m

σ_{min} = Standard deviation of a parcel's bivariate Gaussian distribution along the minor axis, m

σ_t = Standard deviation of a parcel top, m

1. INTRODUCTION

This report presents a discussion of the physical basis of the Airrad fallout prediction system. The equations and algorithms used to model the fallout process are described. Discussions of theory and implementation are presented where appropriate.

2. OVERVIEW

The Airrad computational algorithms are based largely on the SIMFIC (Norment, 1979) and DELFIC (Norment, 1979) fallout prediction codes. The computations can be divided into two general sections. In the first, the initial fireball is divided into parcels, and the ground impact time and ground impact position of each parcel are calculated. In the second section, each parcel's activity is added to a set of grids representing the normalized ground level exposure rate at various times between the start and end of fallout.

Correlations are used to compute the properties of the initial nuclear cloud which is divided into between one and five horizontal, disk-shaped subdivisions, termed wafers. The initial particle population of each wafer is partitioned into discrete size bins, with each resulting family of particles termed a parcel (see Figure 1). The activity associated with each size bin is equally distributed among the set of parcels of that size class.

Representative particles initially at the centers of the top and bottom of each parcel are tracked until ground impact according to the method described in the following paragraph. These particles are known as the top and bottom bounding particles, respectively. Together, they are known as the bounding particles.

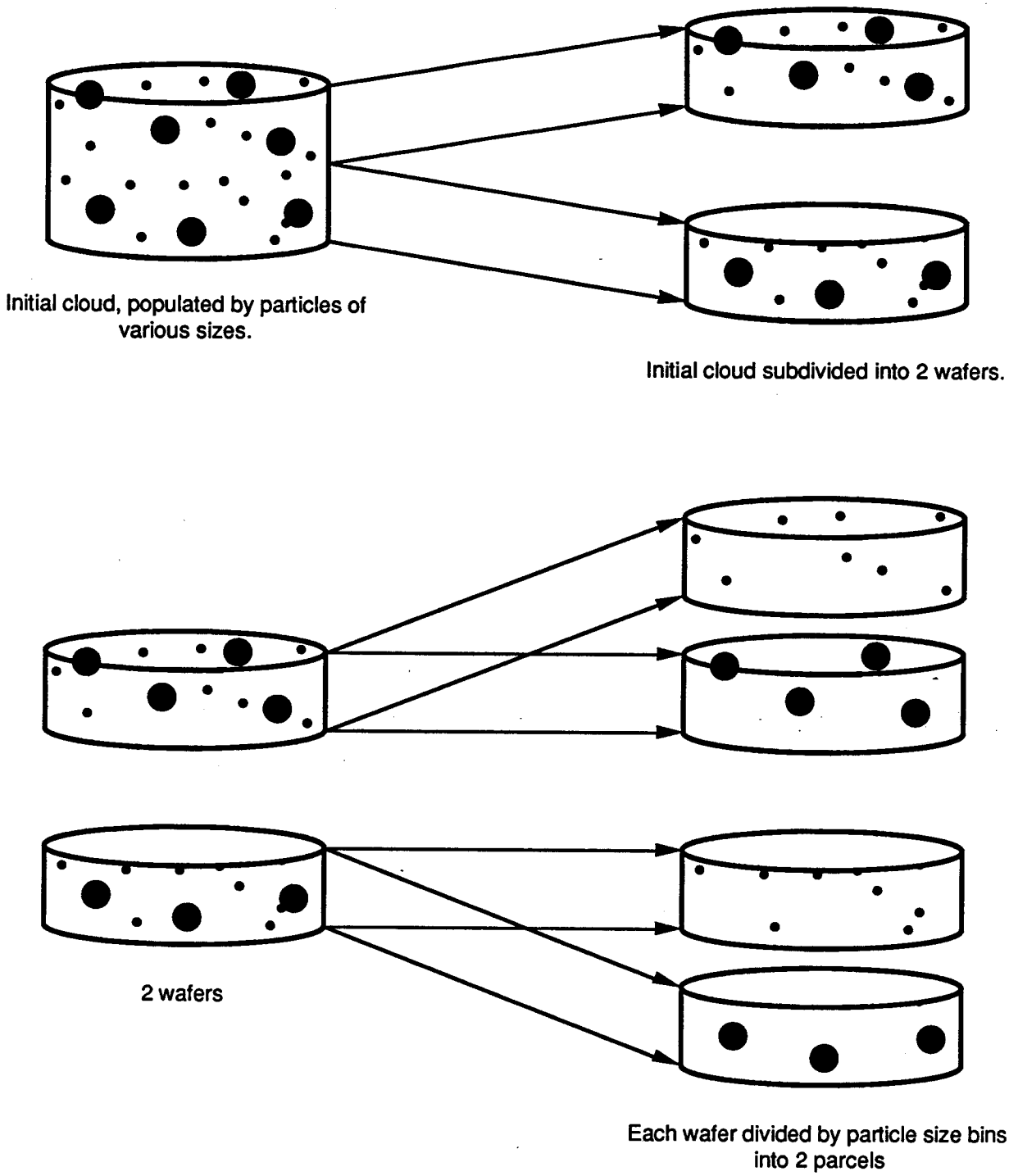

Figure 1. Division of initial cloud into wafers and parcels. In this example, two vertical subdivisions and two particle size bins are used to divide the initial cloud into four parcels. Representative particles initially at the top and bottom of each parcel are tracked to ground impact.

The vertical time-history of the bounding particles for each parcel are computed based on the average fallspeed of particles in the current parcel's size bin and the observation that the altitude of an ascending buoyant cloud tends to be proportional to the square root of the rise time. A table of wind vectors with height is combined with the vertical time-history to produce a function which yields a velocity vector as a function of time for each bounding particle. These functions are integrated with respect to time until ground impact to determine the impact locations of the bounding particles. These locations are taken to be the ground impact positions of the centers of the top and bottom of the parcel which these bounding particle represent. The ground impact locations and times for each parcel are stored for later use.

By considering the contribution of each parcel, it is possible to construct a time-history of the total activity deposition rate. Sixteen times are selected such that an equal amount of activity is deposited between each two adjacent times. These times are termed frame times. A grid of ground level points is associated with each frame time, which contains the footprint of all activity deposited up to that time. These grids are termed frame grids, since they are analogous to the frames of a motion picture which capture the state of the scene being filmed at discrete times.

The activity of each parcel is assumed to have a Gaussian distribution in the horizontal. The standard deviations of the top and bottom of each parcel are computed based on an analytical dispersion algorithm. The ground impact footprint of a parcel is assumed to have a bivariate Gaussian distribution whose foci are the two parcel ground impact locations. The activity of each parcel is added to the appropriate frame grids.

After computation, the 16 frame grids, termed the frame grid set, are stored for future use. A grid representing any of the supported fallout hazard indicators can be quickly computed from the frame grid set.

3. MATHEMATICAL FORMULATION OF AIRRAD

3.1 Internal Units

The Airrad user interface allows data to be entered and results displayed in the user's choice of units. However, with a few exceptions mentioned below, all internal calculations are performed in the MKS-kiloton-Roentgen system. In the sections which follow, distances and heights will always be expressed in meters, times in seconds, velocities in meters per second, yields in kilotons, and exposures in Roentgens.

When the user enters a value in a different system of units, the value is converted into the MKS-kiloton-Roentgen system before it is stored and used. Likewise, an output value is stored in the MKS system and converted to the user's system of units prior to being written to the screen or output file.

The exceptions to the MKS-kiloton-Roentgen rule are as follows.

1. Exposure rates are measured in Roentgens per *hour.*

2. The activity decay equation (eq. 61) assumes that time is in *hours* since the burst.

3.2 Computation of Cloud Properties

The formula in this section represent curve fits to data obtained from observations of nuclear test events at the Nevada and Pacific Test Sites, and from DELFIC simulations.

The initial cloud is defined at a time T_i close to the fireball second temperature maximum

$$T_i = 2.07\ W^{0.19}\ , \qquad (1)$$

where W is the total energy yield of the burst. The cloud stabilization time T_s is found by interpolating on $\log_{10}$ (W) from Table 1.

Table 1

Cloud Stabilization Times[a]

Yield (kt)	Stabilization[b] Time (s)
10^{-3}	421
10^{-2}	421
10^{-1}	381
10	382
10^{1}	422
10^{2}	663
10^{3}	783
10^{4}	787
10^{5}	991

[a] The data in this table were obtained from DELFIC simulations.

[b] Cloud stabilization occurs when ambient dispersion begins to dominate buoyant cloud rise and expansion generated internally by fireball temperature gradients.

The initial radius R_i and stabilized radius R_f are calculated using

$$R_i = 108.0\ W^{1/3} \quad (2)$$

$$R_f = \exp\ (6.7553 + 0.7381\ Y + 0.060308\ Y^2) \quad (3)$$

where $Y = \log_{10}(W)$. The initial cloud base, center, and top altitudes, $Z_{i,B}$, $Z_{i,C}$, and $Z_{i,T}$, respectively, are

$$Z_{i,C} = Z_{gz} + H_b + 90\ W^{1/3} \quad (4)$$

$$Z_{i,B} = Z_{i,C} - 0.66144\ R_i \quad (5)$$

$$Z_{i,T} = Z_{i,C} + 0.66144\ R_i \quad (6)$$

where Z_{gz} is the altitude of ground zero above mean sea level, and H_b is the height of the burst above the ground. The coefficient 0.66144 is derived from the observation that a rising nuclear cloud tends to assume the shape of an oblate spheroid with an average eccentricity of 0.75, as noted by Norment and Woolf (Norment, unpublished). This observation is based on ten test shots with yields ranging from 3.6 kt to 15 Mt. Little variation of eccentricity with height was noted up to the time of cloud stabilization.

The stabilized cloud base and top altitudes, $Z_{f,B}$ and $Z_{f,T}$, respectively, are

$$Z_{f,B} = Z_{gz} + H_b + a\ W^b \quad (7)$$

$$Z_{f,T} = Z_{gz} + H_b + c\ W^d \quad (8)$$

where a, b, c and d are defined in Table 2.

Table 2

Stabilized Cloud Altitude Coefficients

Condition	a	b	c	d
W <= 4.07	2228	0.3463		
W > 4.07	2661	0.2198		
W <= 2.29			3597	0.2553
2.29 < W <= 19.0			3170	0.4077
W > 19			6474	0.1650

The scaled height of burst Z_{scl} is defined as

$$Z_{scl} = \frac{H_b}{W^{1/3}} . \qquad (9)$$

3.3 Activity Fraction Array

The total activity associated with an event is

$$A_{tot} = W_f F_d K \qquad ,R \cdot m^2/hr \quad (10)$$

where W_f is the fission yield of the burst, K is the K-factor for the selected fission type listed in Table 3 and F_d is a scaling factor for the height of the burst above the ground defined as

$$F_d = 0.45345^{(Z_{scl}/19.81)} , \qquad (11)$$

which is based on a curve of deposited activity fraction verses scaled burst height.

Equation (11) is not valid for subsurface ($Z_{scl} < 0$) or free air ($Z_{scl} > \approx 55$) bursts. Its underlying assumption is that the majority of deposited activity is associated with material drawn into the fireball from the ground surface. For free air and subsurface bursts, device casing and crater throw-out material dominate as sources for close-in fallout particles.

Table 3

Activity K-Factors for Selected Fission Types

Fission[a] Type	K-Factor[b] ($R \cdot m^2/hr \cdot kt$)
U233HE	6.3010×10^9
P239HE	6.0830×10^9
P239FI	6.9733×10^9
U235HE	7.2911×10^9
U235FI	7.8643×10^9
U238TN	7.9407×10^9
U238HE	8.2111×10^9

[a] In the Fission Type column, the following symbols have special meanings: U = Uranium, P = Plutonium, HE = High Energy Neutron Fission, FI = Fission Spectrum Neutron Fission, and TN = Thermonuclear Fission.

[b] The K-Factor is a measure of the activity produced by the fission of one kiloton of the selected fission type. If the activity associated with a burst having fission yield W_f and K-Factor K is evenly deposited over a 'large' (edge effects can be ignored) area A, then the normalized H+1 hour exposure rate at a point one meter above the area, is $\frac{W_f K}{A}$ Roentgens per hour.

The activity array $A_{p,i}$ contains the total activity associated with a parcel of size bin i, and is computed using

$$A_{p,i} = \frac{A_{tot}\, A_i}{N_{cd}} \quad , \qquad ,R{\cdot}m^2/hr \quad (12)$$

where N_{cd} is the number of cloud subdivisions (this is the number of wafers into which the initial cloud is divided - the activity is distributed evenly between these wafers) and A_i is the fraction of activity associated with particle size bin i. The activity fractions were computed by DELFIC for a fission yield of 0.5 kt and a fission type representing the average of U238TN and P239HE. A siliceous soil common in continental interiors was assumed in these calculations. As a result, computational accuracy can be expected to deteriorate when predictions are attempted over other burst surfaces, such as water.

Seventy-five particle size bins are known to Airrad. The highest computational accuracy will result from the use of all 75; however, the user can elect to run Airrad using every second, third, or forth particle size bin in order to speed the computational process.

3.4 Average Particle Fallspeed

Following work by Best (1950), the average particle fallspeed through an atmospheric layer can be found by integrating the equation

$$f_z = f_o \exp(bz) \qquad (13)$$

where f_z is the fallspeed at altitude z, f_o is the sea level fallspeed, and

$$b = 2.90 \times 10^{-5};\ 50 < d < 300\ \mu m$$

$$b = 4.05 \times 10^{-5};\ 300 \leq d \leq 6000\ \mu m \quad ,$$

where d is the particle diameter. Although derived for water droplets, this equation gives acceptable results for typical fallout particles.

Equation (13) can be integrated to give the average fallspeed of a particle of size bin i descending from an altitude of Z_1 to Z_2

$$\bar{f} = F_{msl,i} \frac{\exp(b Z_1) - \exp(b Z_2)}{(b Z_1 - b Z_2)} ; Z_1 > Z_2 \qquad (14)$$

where $F_{msl,i}$ is the average mean sea level fallspeed of particles in size bin i. The sea level fallspeeds were calculated using the equations of Beard (1976) and Davies (1945) assuming a particle density of 2600 kg/m^3 *, and are stored in a table. The value of b is 2.90×10^{-5} if $D_{P,i} <$ 300 μm, and 4.05×10^{-5} otherwise, where $D_{P,i}$ is the mass mean diameter of the particles in size bin i, also retrieved from a table.

3.5 Wind Data Processing

Wind data are supplied to Airrad in the form of height-speed-direction triplets. Any combination of the three values may be undefined in any triplet. The wind data processing routines of Airrad perform two major functions.

1. Estimate any undefined wind speeds and directions

* This density is typical of siliceous rock particles. The majority of fallout activity from a surface blast is associated with activated material (rock and soil) drawn into the fireball. The contribution from unfissioned uranium and plutonium is relatively minor.

2. Transform the wind profile from speed-direction format to u-v vector format*

The following is an outline of the algorithm used to estimate undefined wind values. The wind speed and direction at all levels can be found by an application of these rules, which are based upon an average mid-latitude continental wind profile typical of the interior U.S. and Europe. This profile is not applicable within approximately 30° of the equator or near the poles. If the user does not supply any wind data, a default profile will be calculated.

1. If they do not already exist, add new levels at the following nine heights: 2, 100, 1000, 9000, 12000, 13500, 16000, 20000 and 30000 meters above ground level. These heights represents nodes in the vertical wind profile where major shifts in the average wind vector tend to occur. The new levels will have undefined speeds and directions.

2. If an undefined wind speed or direction has defined values above and below it, determine the undefined value by linear interpolation on the closest set of defined values.

---

* The speed-direction format is the standard meteorological format, in which the wind direction is the direction from which the wind blows, measured in degrees clockwise from true north. The u-v vector format assumes that the positive u direction is east and the positive v direction is true north. Thus, a 135° 10 m/s wind could be expressed as (-7.07 u, 7.07 v) m/s in u-v format.

3. Assume all undefined wind directions above 9000 m (≈ 300 mb) are from the west (270°).

4. Assume the wind direction is constant between the top of the boundary layer and 9000 m. The boundary layer height is assumed to be 1000 m. This is an adequate assumption, since the model is not overly sensitive to this parameter.

5. Assume wind veers (turns clockwise) linearly 19° between ground level and the top of the boundary layer. This value was taken from work by Mendenhall (1967).

6. Set the wind speed at levels greater than 9000 m by interpolating on the data presented in Table 4.

Table 4

Average, Mid-latitude Continental Wind Speed Profile[a]

Height (m)	Speed (m/s)
9000	12.3
12000	15.7
13500	13.2
16000	5.8
20000	10.0
30000	20.0

[a]The data in this table are based on records of the average mid-latitude atmospheric circulation patterns during the northern hemisphere summer. To be conservative, summer conditions were used, which results in greater fallout concentration since the wind speed tends to decrease during this period,.

7. Assume the wind speed varies in the boundary layer according to

$$V_z = c\,Z^b \tag{15}$$

$$c = \frac{V_{zk}}{Z_k{}^b} \tag{16}$$

where V_z is the wind speed at height Z, Z_k and V_{zk} are a known height - wind speed pair, and b equals 0.0423. The constant b was calculated from a statistical study of meteorological records from three stations: Amarillo, TX, Peoria, IL, and Grand Junction, CO.

The wind data is transformed from speed-direction to u-v format using

$$U_{w,i} = -S_{w,i} \cos \left[90 - D_{w,i}\right] \quad (17)$$

$$V_{w,i} = -S_{w,i} \sin \left[90 - D_{w,i}\right] \quad (18)$$

where $S_{w,i}$ is the wind speed, $D_{w,i}$ is the wind direction (° cw from true north), and $(U_{w,i}, V_{w,i})$ is the u-v wind vector. The i subscript refers to the i'th wind profile level.

A pair of functions U_w (z), V_w (z) are defined which give the u-v wind vector as a function of altitude by performing a linear interpolation on the $U_{w,i}$ and $V_{w,i}$ tables.

3.6 Division of Initial Cloud into Wafers and Parcels

The dimensions of the initial cloud, $Z_{i,B}$, $Z_{i,T}$ (base and top altitudes), and R_i (radius) are computed in sec. 3.2. At the initial time T_i, all activity-carrying particles in the initial cloud are assumed to have a uniform distribution in the vertical and a Gaussian distribution in the horizontal. Subsequent to this time, each particle assumes its own independent positional time-history owing to its unique diameter (which affects fallspeed) and vertical location in the initial cloud. Note that the wind field is assumed uniform in the horizontal, so that, aside from dispersion, a particle's horizontal location in the initial cloud has no effect on its positional time-history.

The initial cloud is divided into N_{cd} horizontal, disk-shaped subdivisions, termed wafers. The initial particle population of each wafer is further partitioned by discrete size bins, with each resulting family of particles termed a parcel (see Figure 1).

Representative particles initially at the centers of the top and bottom of each parcel are tracked until ground impact. These particles are known as

the top and bottom bounding particles, respectively. Together, they are known as the bounding particles.

The method for determining the ground impact position and time for a bounding particle is discussed in the following sections. For each parcel, these calculations are performed twice, once each for the top and bottom bounding particles.*

3.7 Maximum Height and Time Reached of a Bounding Particle

The maximum height reached, and the time at which this occurs, is computed for the bounding particles of each parcel. The method for performing these computations was taken directly from SIMFIC without modification. The appropriate section of the SIMFIC technical reference manual is reproduced in Appendix A. For each particle size bin, this algorithm is used to compute $z_{m,T}$ (maximum altitude reached by the top bounding particle of the uppermost parcel, in meters above mean sea level), $t_{m,T}$ (the time at which $z_{m,T}$ is reached, in seconds since the burst), $z_{m,B}$, and $t_{m,B}$ (ditto for bottom bounding particle of the lowest parcel). These variables are identical to the variables $z_{m,T}$, $t_{m,T}$, $z_{m,B}$, and $t_{m,B}$ in Appendix A. Formulas (2.4.3) and (2.4.4) in Appendix A are then used to compute Z_m and T_m for the bounding particles of each parcel.

3.8 Vertical Time-History of a Bounding Particle

Parcel boundaries are distributed at equally space intervals throughout the initial cloud's vertical extent. Thus, the initial altitude of a bounding particle at time T_i is given by

---

* In practice, these steps only have to be carried out (NCD + 1) times for the parcels of a particular size bin, since the top bounding particle of every parcel except the highest, is also the bottom bounding particle of the parcel directly above it.

$$Z_i = Z_{i,B} + \frac{i_p}{N_{cd}} (Z_{i,T} - Z_{i,B}) \qquad (19)$$

where i_p is an integer index which is 0 for the lower bounding particle of the lowest parcel, 1 for the upper bounding particle of the lowest parcel and the lower bounding particle of the second parcel, ..., and N_{cd} for the upper bounding particle of the highest parcel (see Figure 2).

The altitude of a rising particle is assumed to be proportional to the square root of its rise time until it reaches its maximum altitude Z_m and time T_m. This has been observed in photometric studies of rising nuclear clouds. Subsequent to T_m, it is assumed to have a constant fallspeed from altitude Z_m to Z_{gz} (ground impact), which is computed using eq. (14). The formulas for the parcel altitude as a function of time are then

$$Z_t = a_0 + a_1 \sqrt{t}\,; \; t < T_m \qquad (20)$$

$$Z_t = b_0 + b_1 t\,; \; t \geq T_m \qquad (21)$$

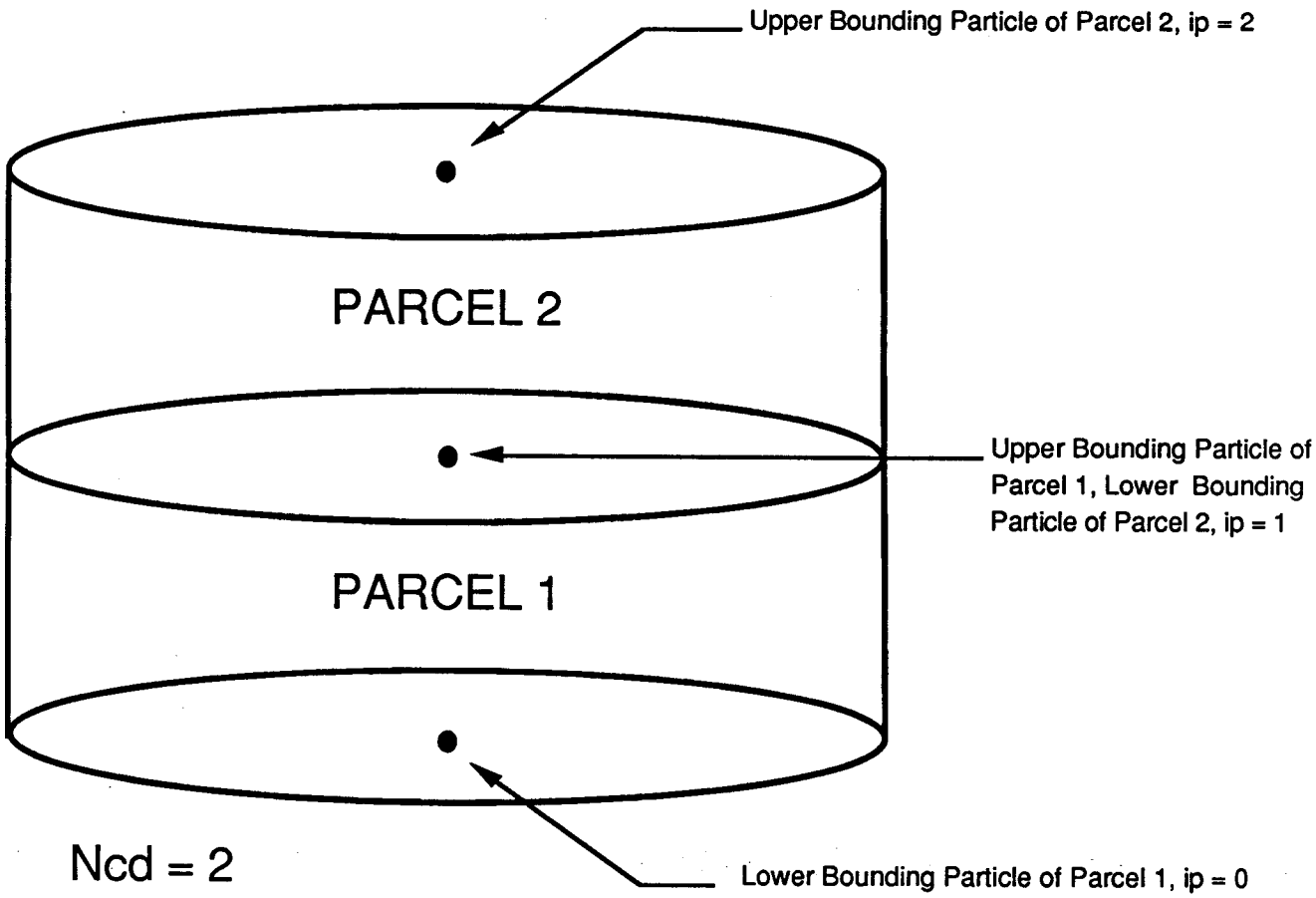

Figure 2. Location of bounding particles and parcel numbering scheme at initial time T_i when all parcels are still in the cloud. In this example, $N_{cd} = 2$, so the initial cloud is divided into two parcels for each particle size bin.

where Z_t is the altitude of the particle above mean sea level, t is the time since the burst (the time between the burst and T_i is small compared to the downwind transport time, and can be ignored), and the coefficients are

$$a_0 = \frac{Z_m - Z_i}{\sqrt{T_m} - \sqrt{T_i}} \qquad (22)$$

$$a_1 = Z_i - a_0 \sqrt{T_i} \qquad (23)$$

$$b_0 = - \langle f \rangle \tag{24}$$

$$b_1 = Z_m + \langle f \rangle T_m \tag{25}$$

where <f> is the average fallspeed of a particle of this size bin falling from Z_m to Z_{gz}. This is computed using eq. (14).

A function Z_p (t) is defined, which incorporates eqs. (20) and (21) above, and returns the altitude of a bounding particle as a function of time t.

The time of ground impact T_g is

$$T_g = T_m + \frac{Z_m - Z_{gz}}{\langle f \rangle} \tag{26}$$

which is the sum of T_m, the time at which the particle reaches its maximum height, and the time required for it to descend to the ground.

Figure 3 illustrates the general vertical time-history of a particle.

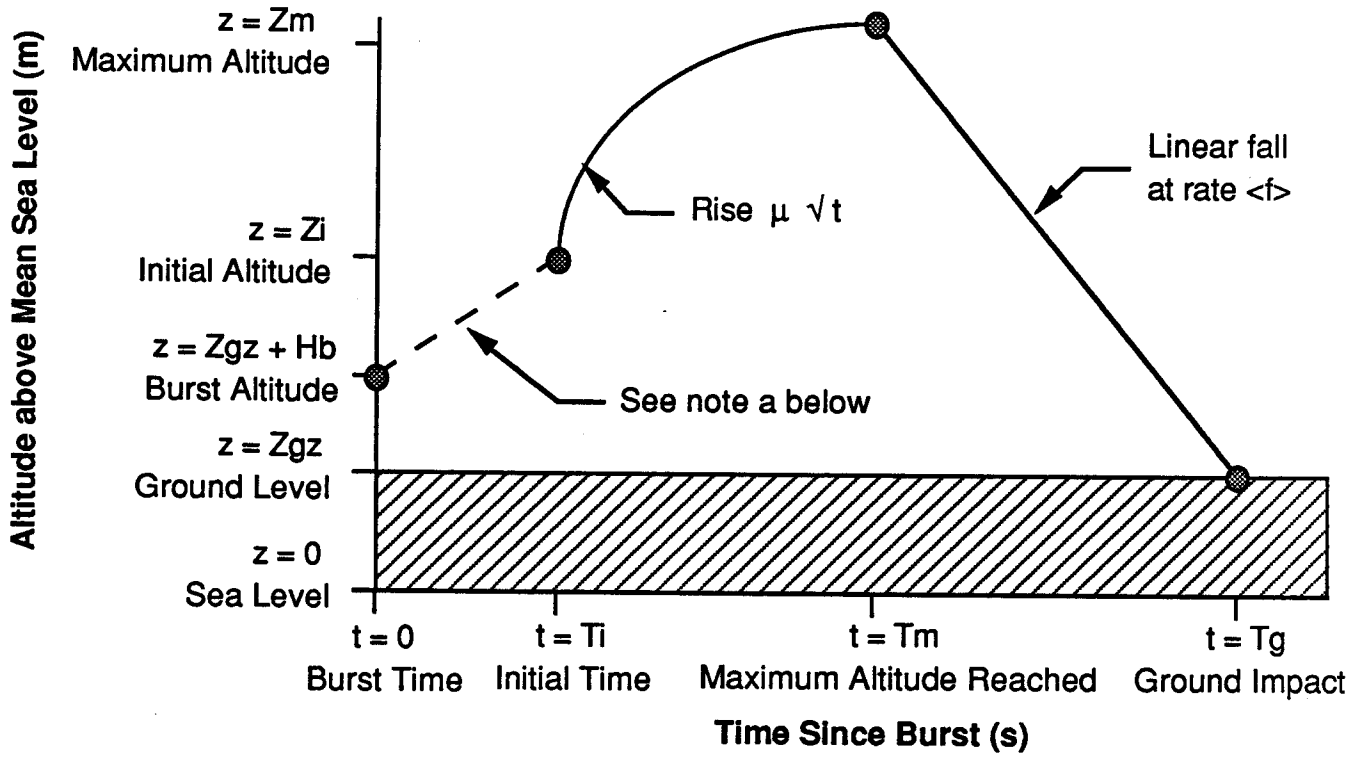

Figure 3. Vertical time-history of a particle from burst time (t = 0) to ground impact (t = T_g).

[a] The initial position is computed analytically from the burst position (0, $Z_{gz} + H_b$), and the burst energy yield W. Ti is on the order of a few seconds, so any horizontal particle advection occurring during this time can be ignored.

3.9 Computation of Parcel Radii

The stabilization radii of the each parcel's top and bottom are computed and stored. Since a bounding particle is associated with the top and bottom of each parcel, there is 1 radii computation for each bounding

particle.* Indeed, the radii computation algorithm makes use of its associated bounding particle's vertical time-history. For convenience, the top and bottom of each parcel will be termed a disk. Each disk is associated with one bounding particle.

Disk growth due to ambient turbulence is ignored prior to the cloud stabilization time T_s. Cloud growth during this period is driven internally by the expanding fireball. As calculated in sec. 3.2, the fireball grows from radius R_i and time T_i, to radius R_f at time T_s. Disks are assumed to grow with the fireball until they drop out of the bottom of the buoyant cloud.

A disk initially at the bottom of the cloud is assumed to immediately drop out of the cloud, and is assigned a stabilization radius R_s of R_i. Higher disks, which are still inside the cloud at stabilization time, receive a stabilization radius of R_f. Intermediate disks, which drop out of the cloud between T_i and T_s, are assigned a stabilization radius intermediate between R_i and R_s by linearly interpolation on height.

$$R_S = R_i + (R_f - R_i) \frac{(Z_S - Z_{S,B})}{(Z_{f,B} - Z_{S,B})} \qquad (27)$$

where Z_S and $Z_{S,B}$ are the stabilization altitudes of the disk in question and the disk initially at the cloud base, respectively. This allows the fallout presents in the nuclear cloud stem to be accurately modeled. The

* As before, in practice, these steps only have to be carried out (NCD + 1) times for the parcels of a particular size bin, since the top disk of every parcel except the highest, is also the bottom disk of the parcel directly above it.

stem forms naturally as a consequence of particles dropping out of the bottom of the expanding fireball before it reaches its final size. The stabilization altitudes are calculated using

$$Z_s = Z_m - \langle f \rangle (T_s - T_m) \quad (28)$$

$$Z_{s,B} = z_{m,B} - \langle f \rangle (T_s - t_{m,B}) \quad (29)$$

where <f> is the average fallspeed of a particle of this size bin calculated by the method in sec. 3.4, Z_m and $z_{m,B}$ are the maximum altitudes reached by these two disks and T_m and $t_{m,B}$ are the times when the maximum altitudes were reached.

3.10 Parcel Advection

In sec. 3.5, a pair of functions U_w (z), V_w (z) were defined, which return the u and v components of the horizontal wind vector as a function of altitude (the wind field is assumed uniform in the horizontal). A function Z_p (t), defined in sec. 3.8, returns the altitude of a particle as a function of the time since the burst. These functions can be combined to yield functions giving the wind vector experienced by a particle as a function of time, which can be integrated to yield the ground impact location of the particle

$$X_g = \int_{T_i}^{T_g} U_w(Z_p(t))\, dt + X_{gz} \quad (30)$$

$$Y_g = \int_{T_i}^{T_g} V_w(Z_p(t))\, dt + Y_{gz} \quad (31)$$

where (X_g, Y_g) are the ground impact coordinates of this particle (meters east and north), and (X_{gz}, Y_{gz}) are the coordinates of ground zero. Airrad

uses a numerical integration routine to evaluate these integrals. Note that advection occurring between t=0 and $t=T_i$ is ignored. T_i is typically less than 20 seconds; significant transport could not occur in this time.

3.11 Computing Grid Frame Times

Recall that the ground impact times of the bounding particles for each parcel have been computed and stored (sec. 3.8). Also recall that the total amount of activity associated with each parcel has been computed (sec. 3.3). If it is assumed that the activity deposition rate is constant between the bounding particle ground impact times, the deposition time-history of a parcel is

$$\frac{D}{dt} = 0 \; ; \quad t < T_{g,b} \qquad ,(R \cdot m^2/hr)/s \quad (32)$$

$$\frac{D}{dt} = \frac{A_{p,i}}{T_{g,t} - T_{g,b}} \; ; \quad T_{g,b} \leq t \leq T_{g,t} \qquad ,(R \cdot m^2/hr)/s \quad (33)$$

$$\frac{D}{dt} = 0 \; ; \quad t > T_{g,t} \qquad ,(R \cdot m^2/hr)/s \quad (34)$$

where $A_{p,i}$ is the total activity associated with a parcel of this size class, $T_{g,t}$ and $T_{g,b}$ are the ground impact times of this parcel and $\frac{D}{dt}$ is the activity deposition rate at time t. With this system of units, $\frac{D}{dt} = 1$ implies that the activity deposited on a one m^2 area in a one second time interval would produce an exposure rate of one R/hr (see note b below Table 3).

By summing the deposition time-histories of every parcel, it is possible to construct a time-history of the total activity deposition rate. Sixteen frame times are selected such that

1. One frame time is set to the time of first fallout.*

2. One frame time is set to the time of last fallout.

3. The remaining frame times are set such that an equal amount of activity is deposited between any two adjacent pairs of frame times.

Frame times are expressed in seconds since the burst.

A grid of ground level points is associated with each frame time. These grids are termed frame grids, since they are analogous to the frames of a motion picture, which capture the state of the scene being filmed at discrete times.

3.12 Association Between Frame Grid Points and User Coordinates

Four coefficients are defined which allow a grid index [i, j] to be mapped to a corresponding user coordinate pair (X, Y) with

$$X = C_{x0} + C_{x1}\, i \tag{35}$$

$$Y = C_{y0} + C_{y1}\, j \tag{36}$$

where

---

* The grid associated with this frame time will be all zeros, since it represents the time when fallout is just beginning. This may seem unnecessary. However, it simplifies later algorithms, and will facilitate changes if a multiple burst capability is ever added to Airrad.

$$C_{x0} = O_{G,x} - S_{G,x} \quad (37)$$

$$C_{y0} = O_{G,y} - S_{G,y} \quad (38)$$

$$C_{x1} = S_{G,x} \quad (39)$$

$$C_{y1} = S_{G,y} \quad (40)$$

where $(O_{G,x}, O_{G,y})$ are the location of the grid origin (grid point [1, 1]) in user coordinates (meters east and north from a user selected origin) and $(S_{G,x}, S_{G,y})$ are the distances between adjacent grid points (m) in the x (east) and y (north) directions. Figure 4 illustrates the various grid features.

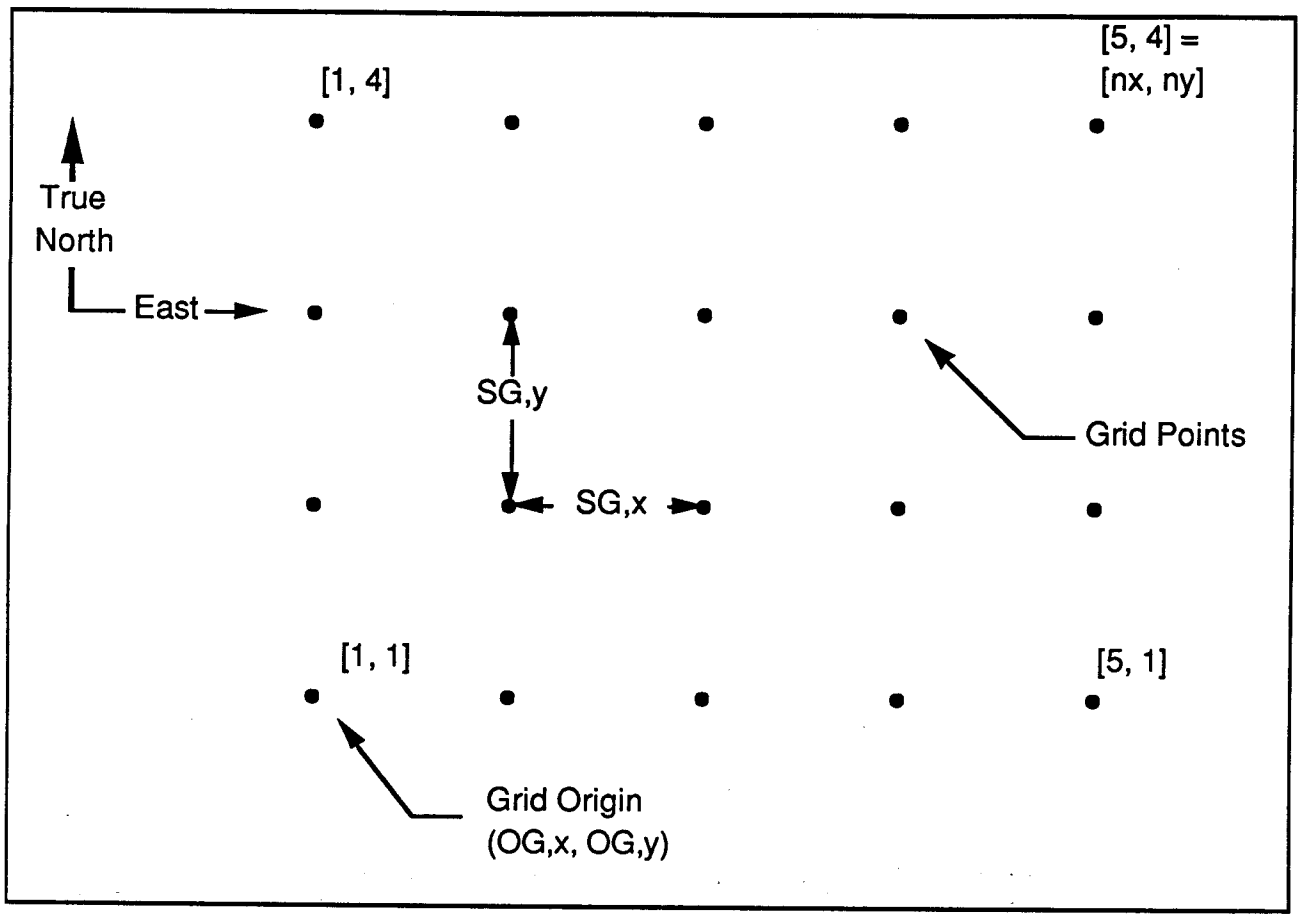

Figure 4. Features of a frame grid. $O_{G,x}$, $O_{G,y}$ (user coordinates of grid origin [1, 1]), $S_{G,x}$, $S_{G,y}$ (grid spacing in x and y directions), and n_x, n_y (number of grid points in the x and y directions) are user supplied parameters. All frames grids are spatially identical, differing only in their frame time. In this example, $n_x = 5$ and $n_y = 4$.

3.13 Calculation of a Disk's Ground Impact Standard Deviation

Following DELFIC and SIMFIC, which are based on work by Walton (1973), a disk is assumed to have a Gaussian distribution in the horizontal at time t with variance

$$\sigma(t)^2 = \left[\sigma(t_s)^{2/3} + \frac{2}{3}\varepsilon^{1/3}(t - T_s)\right]^3$$

$$; \sigma(t_s) \leq \sigma(t) \leq \sigma_l \qquad (41)$$

$$\sigma(t)^2 = \sigma_I^2 \left[2(t - T_s) \left(\frac{\varepsilon}{\sigma_I^2}\right)^{1/3} + 3 \left(\frac{\sigma(ts)^2}{\sigma_I^2} \right)^{1/3} - 2 \right]$$

$$; \sigma(t) > \sigma_I \qquad (42)$$

where σ_I^2 is the disk variance when the dispersion rate becomes constant, taken to be 10^9 m^2, $\sigma(t_s)$ is the standard deviation of the disk at stabilization time, taken to be $\frac{1}{2}R_s$, and ε, the turbulence energy dissipation rate, can be computed using Wilkens' (1963) approximation

$$\varepsilon = \frac{0.06}{(Z_m - Z_{gz})} \quad , m^{-1} \qquad (43)$$

The ground impact standard deviation of a disk is defined as

$$\sigma_G = \sqrt{\sigma(T_g)^2} \qquad (44)$$

3.14 Distribution of a Parcel's Activity Over a Grid of Points

A work grid, G, with the same parameters as the frame grid set is defined. For each parcel, the total activity associated with this parcel is deposited on G using a bivariate Gaussian distribution (hereafter referred to simply as the distribution) with foci at (X_t, Y_t) and (X_b, Y_b) using the method outlined in the remainder of this section. Figure 5 illustrates this process, and is a useful reference for the remainder of this section.

Recall that the following information has been computed and stored for each parcel.

X_t, Y_t	Ground impact location, (X_g, Y_g), of the parcel top
T_t	Time of ground impact of the parcel top

X_b, Y_b Ground impact location, (X_g, Y_g), of the parcel base

T_b Time of ground impact of the parcel base

$A_{p,i}$ Activity associated with this parcel (i refers to this parcel's particle size bin)

The standard deviations of the top and bottom of a parcel can be calculated using the method outlined in sec. 3.13.

σ_t Standard deviation at time of ground impact of the parcel's top.

σ_b Standard deviation at time of ground impact of the parcel's base.

The x and y components of the distance between the ground impact positions are

$$\Delta X = X_t - X_b \tag{45}$$

$$\Delta Y = Y_t - Y_b \ , \tag{46}$$

while the straight-line distance is

$$r = \sqrt{\Delta X^2 + \Delta Y^2} \ . \tag{47}$$

The point half way between the two ground impact positions,

$$X_p = \frac{X_t + X_b}{2} \tag{48}$$

$$Y_p = \frac{Y_t + Y_b}{2} \ , \tag{49}$$

is also taken to be the center of the distribution associated with this parcel. The standard deviations of the distribution along the major and minor axes* are

$$\sigma_{maj} = \frac{|\sigma_t + \sigma_b + r|}{2} \tag{50}$$

$$\sigma_{min} = \sqrt{\sigma_t \sigma_b} \ . \tag{51}$$

If θ is the angle of the major axis of this parcel's distribution, measured counterclockwise from east, then θ's cosine and sine may be found with

$$\cos\theta = \frac{\Delta X}{r} \tag{52}$$

$$\sin\theta = \frac{\Delta Y}{r} \ . \tag{53}$$

For each point in the work grid G_{ij}, the corresponding user coordinates (X, Y) are

$$X = C_{x0} + C_{x1}\, i \tag{54}$$

$$Y = C_{y0} + C_{y1}\, j \ . \tag{55}$$

---

* In the majority of cases, the terms major and minor will be correct. Occasionally two parcels may impact very close to each other. In this case, the minor axis, as computed in these formula, may actually be longer that the major axis. However, the formula will still function correctly, and the terms major and minor are appropriate for most cases.

The components of the distance between the grid point and the center of the distribution, may be found using

$$\Delta_{maj} = \cos\theta\,(X - X_p) + \sin\theta\,(Y - Y_p) \tag{56}$$

$$\Delta_{min} = \cos\theta\,(Y - Y_p) - \sin\theta\,(X - X_p)\ . \tag{57}$$

Note that this is in a rotated coordinate system, with axes parallel to the distribution's major and minor axes.

The H + 1 hour normalized exposure rate at the grid point G_{ij} is with the standard bivariate Gaussian function

$$G_{ij} = \frac{A_{p,i}}{2\,\pi\,\sigma_{maj}\,\sigma_{min}} \exp\left[\frac{-\Delta^2_{maj}}{2\,\sigma^2_{maj}} + \frac{-\Delta^2_{min}}{2\,\sigma^2_{min}}\right]. \tag{58}$$

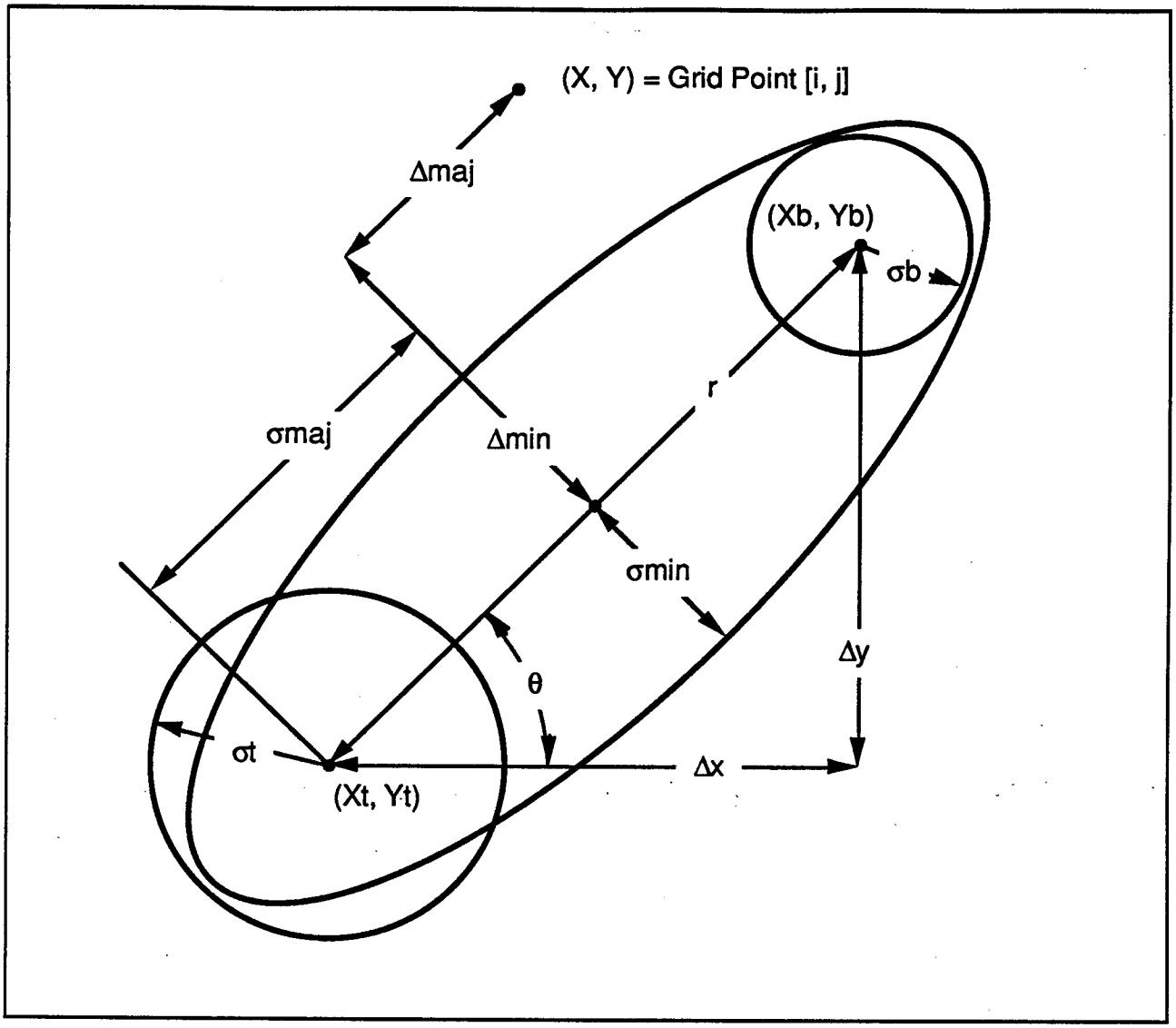

Figure 5. Addition of a parcel's activity to a grid, illustrating the major parameters defined in sec. 3.14.

3.15 Summation of Parcel Activity Contributions on the Frame Grids

For each parcel, the work grid G is computed as outlined in sec. 3.14, and then added to the appropriate set of frame grids. The underlying assumption is that the deposition rate of a parcel is constant from the time of ground impact of the parcel base, to the time of impact of the parcel top.

For each grid point [i, j] in each frame grid t

$$F_{tij} = F_{tij} + G_{ij} \; ; \; T_{F,t} \geq T_t \tag{59}$$

$$F_{tij} = F_{tij} + \frac{T_{F,t} - T_b}{T_t - T_b} G_{ij} \; ; \; T_b < T_{F,t} < T_t \tag{60}$$

where F_{tij} is the content of the [i, j] cell of frame grid t, $T_{F,t}$ is the frame time associated with frame grid t, and T_t and T_b are the ground impact times of this parcel's bounding particles.

3.16 Computation of Hazard Indicators from Frame Grids

The frame grid set, once computed, can be used to quickly calculate any of the common fallout hazard indicators. In the following discussion, H_{ij} is the hazard indicator under discussion at grid location [i, j], F_{tij} is the value of grid point [i, j] of frame grid t, and $T_{F,t}$ is the frame time of frame grid t. The frame times run in sequence, with $T_{F,1}$ being the earliest (time of first fallout), and $T_{F,n}$ being the latest (time of last fallout). In this section, all times are expressed in hours since the burst.

The activity exposure rate is assumed to decay according to

$$R_t = R_{H+1} \, t^{-1.26} \tag{61}$$

where R_t is the exposure rate at time t, R_{H+1} is the exposure rate at H + 1 hours (i.e., one hour since the burst), and t is the time since the burst in hours. This differs from the more commonly seen formula, which uses a power of -1.2. The value of -1.26 was selected because it more closely represents observed data during the critical period of one to fifteen hours after the burst. This is the period in which Airrad is expected to have its' greatest utility. Both -1.2 and -1.26 give acceptable results over the period from 10 minutes to several months after the blast.

A normalized hazard indicator assumes that all fallout has arrived by a specified time t. Since all fallout is assumed to be deposited at time $T_{F,n}$, the normalized exposure rate at a time t (t is typically one hour) is

$$H_{ij} = t^{-1.26} F_{nij} \tag{62}$$

where the n subscript on F refers to the last (latest in time) frame grid. This formula also gives the actual exposure rate for any time after last fallout ($t > T_{F,n}$).

The actual exposure rate at any time t between the time of first and time of last fallout ($T_{F,1} \leq t \leq T_{F,n}$), may be found by linearly interpolating on time between the two frame grids which bracket t,

$$Hij = t^{-1.26} (C_k F_{kij} + C_{k+1} F_{(k+1)ij}) \tag{63}$$

where t is the time in hours, k and k+1 refer to the two frame grids whose frame times bracket t (i.e., $T_{F,k} \leq t \leq T_{F,k+1}$), and

$$C_k = \frac{T_{F,k+1} - t}{T_{F,k+1} - T_{F,k}} \tag{64}$$

$$C_{k+1} = \frac{t - T_{F,k}}{T_{F,k+1} - T_{F,k}} . \tag{65}$$

The exposure rate at any time before first fallout ($t < T_{F,1}$) is assumed to be zero.

A function R_{ij} (t) can be defined using eqs. (62)-(65), which gives the exposure rate as a function of time t. This can be integrated to give the total dosage D_{ij} between two times t_1 and t_2*

$$D_{ij} = \int_{t_1}^{t_2} R_{ij}(t)\, dt \quad . \tag{66}$$

The time of first fallout at a point [i, j] can be conservatively estimated as the frame time just before fallout begins (i.e., $T_{F,t}$ such that $F_{tij} = 0$ and $F_{(t+1)ij} > 0$). Similarly, the time of last fallout may be estimated as the first frame time after fallout ends (i.e., $T_{F,t}$ such that $F_{(t-1)ij} <> F_{nij}$ and $F_{tij} = F_{nij}$).

* In practice, eq. (64) is not numerically integrated: a more efficient summing algorithm is used in Airrad. However, this algorithm is mathematically equivalent to eq. (64).

APPENDIX A

THE SIMFIC METHOD FOR COMPUTING MAXIMUM PARTICLE ALTITUDES

The method for computing the maximum height reached by a parcel's bounding particles and the time at which this occurs was taken from the SIMFIC fallout prediction code without modification. The appropriate section of the SIMFIC technical reference manual is reproduced here.

2.2 VERTICAL TRAJECTORY EQUATIONS

In accord with the proportionality of cloud altitude with the square root of time, the altitudes of cloud (cap) base and top, z_B and z_T, at time t are given by linear interpolation on $\sqrt{t}$ between initial and final altitudes, $z_{B,i}$, $z_{T,i}$ and $z_{B,s}$, $z_{T,s}$, as

$$z_B = z_{B,i} + \frac{\sqrt{t} - \sqrt{t_i}}{\sqrt{t_s} - \sqrt{t_i}} (z_{B,s} - z_{B,i}) \qquad (2.2.1B)$$

$$z_T = z_{T,i} + \frac{\sqrt{t} - \sqrt{t_i}}{\sqrt{t_s} - \sqrt{t_i}} (z_{T,s} - z_{T,i}) \qquad (2.2.1T)$$

where the cloud rise is taken to begin at time t_i after detonation and end at time t_s. Differentiation of equations (2.2.1B and 2.2.1T) give the base and top velocities

$$u_B = \frac{(z_{B,s} - z_{B,i})}{2\sqrt{t}\,(\sqrt{t_s} - \sqrt{t_i})} \qquad (2.2.2B)$$

$$u_T = \frac{(z_{T,s} - z_{T,i})}{2\sqrt{t}\,(\sqrt{t_s} - \sqrt{t_i})} \qquad (2.2.2T)$$

Following the procedure used in DELFIC, which apparently follows Anderson, we assume a linear variation of rise speed inside the cloud between z_B and z_T. Thus the vertical velocity of an in-cloud particle at altitude z with settling speed f is

$$\frac{dz}{dt} = u_B + \frac{(z - z_B)(u_T - u_B)}{(z_T - z_B)} - f; \quad z > z_B, \quad t < t_s \qquad (2.2.3)$$

Also following DELFIC, we assume that upward drift velocity of air below the cloud decreases linearly with distance from the cloud base, which gives for the below-cloud particle velocity

$$\frac{dz}{dt} = \frac{z u_B}{z_B} - f; \quad z \le z_B, \; t < t_s \; . \qquad (2.2.4)$$

At this point it is expedient to normalize the variables as follows:

$$\zeta = \frac{z}{(z_{B,s} - z_{B,i})} \qquad (2.2.5)$$

$$\tau = \frac{\sqrt{t}}{(\sqrt{t_s} - \sqrt{t_i})} \qquad (2.2.6)$$

$$v = \frac{d\zeta}{d\tau} = 2\tau u \frac{(\sqrt{t_s} - \sqrt{t_i})^2}{(z_{B,s} - z_{B,i})} \; , \qquad (2.2.7)$$

and a normalized, average settling speed is defined as

This page reproduced from DNA 5193F:
"SIMFIC: A Simple, Efficient Fallout Prediction Model."

$$\hat{f} = \langle f \rangle \left(\sqrt{t_s} - \sqrt{t_i} \right)^2 (z_{B,s} - z_{B,i}) \quad . \qquad (2.2.8)$$

In normalized form the equations above become

$$\zeta_B = \zeta_{B,i} + \tau - \tau_i \qquad (2.2.1Bn)$$

$$\zeta_T = \zeta_{T,i} + (\tau - \tau_i)(\zeta_{T,s} - \zeta_{T,i}) \qquad (2.2.1Tn)$$

$$v_B = 1 \qquad (2.2.2Bn)$$

$$v_T = \zeta_{T,s} - \zeta_{T,i} \quad . \qquad (2.2.2Tn)$$

For the in-cloud particle we have

$$v = 1 \mp \frac{(\zeta - \zeta_{B,i} - \tau + \tau_i)}{(\tau - \tau_i + a)} - 2\tau\hat{f}; \ \zeta > \zeta_B, \ \tau < \tau_s \qquad (2.2.3n)$$

where

$$a = \frac{(\zeta_{T,i} - \zeta_{B,i})}{(\zeta_{T,s} - \zeta_{T,i} - 1)} \ , \qquad (2.2.9)$$

and for the below-cloud particle we have

$$v = \frac{\zeta}{(\tau - \tau_i + \zeta_{B,i})} - 2\tau\hat{f}; \ \zeta \le \zeta_B, \ \tau < \tau_s \quad . \qquad (2.2.4n)$$

This page reproduced from DNA 5193F:
"SIMFIC: A Simple, Efficient Fallout Prediction Model."

After the cloud stops rising we have

$$v = -2\tau\hat{f};\ \tau > \tau s\ . \qquad (2.2.10)$$

Equations (2.2.3n), (2.2.4n) and (2.2.10) can be integrated to give the vertical trajectory equations:

In-cloud

$$\zeta - \zeta_i = \frac{(a + \zeta_i + \zeta_{B,i})(\tau - \tau_i)}{a} - 2\hat{f}(\tau - \tau_i + a)$$

$$\left[\tau - \tau_i + (\tau_i - a)\ \ln\left(\frac{\tau - \tau_i + a}{a}\right)\right];\ \zeta > \zeta_B,\ \tau < \tau_o,\ \tau < \tau_s$$

(2.2.11)

Below-cloud

$$\zeta - \zeta_o = \frac{\zeta_o(\tau - \tau_o)}{(\tau_o - \tau_i + \zeta_{B,i})} - 2\hat{f}(\tau - \tau_i + \zeta_{B,i})$$

$$\left[\tau - \tau_o + (\tau_i - \zeta_{B,i})\ \ln\left(\frac{\tau - \tau_i + \zeta_{B,i}}{\tau_o - \tau_i + \zeta_{B,i}}\right)\right];\ \zeta \le \zeta_B,\ \tau_o < \tau < \tau_s$$

(2.2.12)

After completion of cloud rise

$$\zeta = \zeta_{\tau=\tau s} - \hat{f}\,(\tau^2 - \tau_s^2);\ \tau > \tau_s\ . \qquad (2.2.13)$$

Here τ_o and ζ_o are the time and altitude of separation of the particle from the cloud cap. Next we address the problem of the determination of τ_o and ζ_o.

TIME AND ALTITUDE OF PARTICLE SEPARATION FROM THE CLOUD

Fallout from the cloud cap occurs when $\zeta = \zeta_B$. By substituting eq. (2.2.1Bn) into the left side of eq. (2.2.11) and manipulating the result algebraically we arrive at

$$\tau_o - \tau_i + a + (\tau_i - a)\ \ln(\tau_o - \tau_i + a) = \frac{(\zeta_i - \zeta_{B,i})}{2\ a\ \hat{f}} + (\tau_i - a)\ \ln(a) + a\ . \qquad (2.3.1)$$

This has the form

$$\xi + b \ln(\xi) = c \qquad (2.3.2)$$

which can be solved for ξ by Newton iteration. Then $\tau_o = \xi + \tau_i - a$, and ζ_o is found by substituting τ_o into eq. (2.2.1Bn).

This page reproduced from DNA 5193F:
"SIMFIC: A Simple, Efficient Fallout Prediction Model."

MAXIMUM PARTICLE HEIGHT

The quantities actually used in the fallout prediction are the maximum altitude of the particle and the time this altitude is reached.

For in-cloud particles, set the left side of eq. (2.2.3n) to zero, solve for ζ_m, the maximum altitude, in terms of τ_m, the time at which ζ_m is reached,

$$\zeta_m = \zeta_{B,i} - a + 2\,\tau_m\,\hat{f}\,(\tau_m - \tau_i + a) \qquad (2.4.1)$$

and substitute this into eq. (2.2.11). After algebraic manipulation we arrive at an equation of the same form as eq. (2.3.2), but for which

$$\xi = \tau_m - \tau_i + a$$

$$b = \frac{(\tau_i - a)}{2}$$

$$c = \frac{a + \zeta_i - \zeta_{B,i}}{4\,\hat{f}\,a} + b \ln (a) + \frac{\tau_i}{2} + a \ .$$

As with eq. (2.3.2) this is solved for ξ by Newton iteration, τ_m is recovered from ξ, and ζ_m is found by substitution of τ_m into eq. (2.4.1).

For below-cloud particles, set the left side of eq. (2.2.4n) to zero, solve for ζ_m in terms of τ_m,

This page reproduced from DNA 5193F:
"SIMFIC: A Simple, Efficient Fallout Prediction Model."

$$\zeta_m = 2\,\tau_m\,\hat{f}\,(\tau_m - \tau_i + \zeta_{B,i}) \qquad (2.4.2)$$

substitute this into eq. (2.2.12), and after algebraic manipulation we again arrive at an equation of the form of eq. (2.3.2), but with

$$\xi = \tau_m - \tau_i + \zeta_{B,i}$$

$$b = \frac{\tau_i - \zeta_{B,i}}{2}$$

$$c = \frac{\zeta_o}{\left[4\,\hat{f}\,(\tau_o - \tau_i + \zeta_{B,i})\right]} + \frac{\tau_o}{2} + b \ln (\tau_o - \tau_i + \zeta_{B,i}) - \tau_i + \zeta_{B,i} .$$

As before this is solved for ξ by Newton iteration, etc.

To select appropriate values for τ_m, ζ_m various possibilities must be examined. (Subscripts IC and BC denote in-cloud and below-cloud):

1. If $\tau_o > \tau_s$ and $\tau_{m|IC} > \tau_s$, then set $\tau_m = \tau_s$ and calculate ζ_m by substitution of τ_s into eq. (2.2.11).

2. If $\tau_o > \tau_s$ and $\tau_{m|IC} \leq \tau_s$, then use $(\tau m, \zeta m)_{IC}$.

3. If $\tau_o \leq \tau_s$ and $\tau_s \geq \tau_{m|BC} > \tau_o$ and $\zeta_{m|BC} > \zeta_{m|IC}$ or $\tau_{m|IC} > \tau_o$ use $(\tau_m, \zeta_m)_{BC}$.

4. If $\tau_o \leq \tau_s$ and $\tau_{m|BC} > \tau_o$ and $\zeta_{m|BC} > \zeta_{m|IC}$ or $\tau_{m|IC} > \tau_o$, but $\tau_{m|BC} > \tau_s$ then set $\tau_m = \tau_s$ and compute ζ_m by substitution of τ_s into eq. (2.2.12).

To save computer time, z_m and t_m are computes only for the particles at the base and top of the initial cloud for each particle size. For particles at intermediate initial positions, the following interpolation formula gives acceptable results

$$t_m = t_{m,B} + k^{0.85} (t_{m,T} - t_{m,B}) \qquad (2.4.3)$$

and

$$z_m = z_{m,B} + k^{0.85} (z_{m,T} - z_{m,B}) \qquad (2.4.4)$$

where

$$k = \frac{(z_i - z_{B,i})}{(z_{T,i} - z_{B,i})} .$$

BIBLIOGRAPHY

K. V. Beard. Terminal Velocity and Shape of Cloud and Precipitation Drops Aloft. J. Atm. Sci. 33, 851. 1976. (Particle Fallspeed Formula)

A. C. Best. Empirical Formulae for the Terminal Velocity of Water Drops Falling Through the Atmosphere. Quart. J. Roy. Meteor. Soc. 76, 302. 1950. (Particle Fallspeed Formula)

H. Boogaard. The Mean Circulation of the Tropical and Subtropical Atmosphere - July. NCAR Technical Note NCAR-TN/118+STR. National Center for Atmospheric Research, Boulder, CO. September, 1977. (Estimation Algorithm for Missing Wind Data)

Stephen P. Conners. Aircrew Dose and Engine Dust Ingestion From Nuclear Cloud Penetration. MS Thesis. Air Force Institute of Technology, Wright-Patterson AFB, OH. March, 1985. (Data on Effects of Airborne Activity)

C. N. Davies. Definitive Equations for the Fluid Resistance of Spheres. Proc. Phys. Soc. (London) 57, 259. 1945. (Particle Fallspeed Formula)

Samuel Glasstone and Philip J. Dolan. The Effects of Nuclear Weapons (3rd ed). U.S. Government Printing Office, Washington, DC. 1977. (General Radiation Physics, Atmospheric Attenuation Function)

Howard A. Hawthorne, Editor. Compilation of Local Fallout Data From Test Detonations 1945-1962 Extracted From DASA 1251. DNA 1251-EX. General Electric Company-TEMPO, Santa Barbara, CA. May 1979. (Computational Engine Validation Data)

David D. Houghton, Editor. Handbook of Applied Meteorology. John Wiley & Sons, Inc. 1985. (Estimation Algorithm for Missing Wind Data)

Robert J. List, Editor. Smithsonian Meteorological Tables (6th rev ed). (Estimation Algorithm for Missing Wind Data)

B. R. Mendenhall. A Statistical Study of Frictional Wind Veering in the Planetary Boundary Layer. Colorado State University, Atmos. Sci. Pap. No. 116. 1967. (Estimation Algorithm for Missing Wind Data)

Hillyer G. Norment. Delfic: Department of Defense Fallout Prediction System. DNA 5159F. Atmospheric Science Associates, Bedford, MA. December 1979. (Computational Engine Algorithms and Data)

Hillyer G. Norment. DNAF-1: An Analytical Fallout Prediction Model and Code. DNA 6168F. Atmospheric Sciences Associates, Bedford, MA. October 1981. (Computational Engine Algorithms)

Hillyer G. Norment. Simfic: A Simple, Efficient Fallout Prediction Model. DNA 5193F. Atmospheric Science Associates, Bedford, MA. December 1979. (Computational Engine Algorithms and Data)

Hillyer G. Norment and W. Woolf. Studies of Nuclear Cloud Rise and Growth. Technical Operations, Inc. Unpublished. (Nuclear Cloud Growth Algorithms)

Darryl Randerson, Editor. Atmospheric Science and Power Production. DOE/TIC 27601. Technical Information Center, Springfield, VA. July, 1984. (Estimation Algorithm for Missing Wind Data, Nuclear Cloud Dispersion Algorithm)

J. J. Walton. Scale Dependent Diffusion. J. Appl. Meteor. 12. 547. 1973. (Nuclear Cloud Dispersion Algorithm)

E. M. Wilkins. Decay Rates for Turbulent Energy Throughout the Atmosphere.. J. Atm. Sci. 20. 473. 1963. (Nuclear Cloud Dispersion Algorithm)